The Cryosphere Discuss., 6, 2931–2959, 2012
www.the-cryosphere-discuss.net/6/2931/2012/
doi:10.5194/tcd-6-2931-2012

The Cryosphere Discussions

Constraining projections of summer Arctic sea ice

F. Massonnet[1], T. Fichefet[1], H. Goosse[1], C. M. Bitz[2], G. Philippon-Berthier[1,3], M. M. Holland[4], and P.-Y. Barriat[1]

[1]Georges Lemaître Centre for Earth and Climate Research, Earth and Life Institute, Université catholique de Louvain, Louvain-la-Neuve, Belgium
[2]Department of Atmospheric Sciences, University of Washington, Seattle, WA, USA
[3]Laboratoire des Sciences du Climat et de l'Environnement, Gif-sur-Yvette, France
[4]National Center for Atmospheric Research, Boulder, CO, USA

Received: 7 July 2012 – Accepted: 17 July 2012 – Published: 27 July 2012

Correspondence to: F. Massonnet (francois.massonnet@uclouvain.be)

Published by Copernicus Publications on behalf of the European Geosciences Union.

Abstract

We examine the recent (1979–2010) and future (2011–2100) characteristics of the summer Arctic sea ice cover as simulated by 29 Earth system and general circulation models from the Coupled Model Intercomparison Project, phase 5 (CMIP5). As was the case with CMIP3, a large inter-model spread persists in the simulated summer sea ice losses over the 21st century for a given forcing scenario. The initial 1979–2010 sea ice properties (including the sea ice extent, thickness distribution and volume characteristics) of each CMIP5 model are discussed as potential constraints on the September sea ice extent (SSIE) projections. Our results suggest first that the SSIE anomalies (compared to the 1979–2010 model SSIE) are related in a complicated manner to the initial 1979–2010 sea ice model characteristics, due to the large diversity of the CMIP5 population (at a given time, some models are in an ice-free state while others are still on the track of ice loss). In a new diagram (that does not consider the time as an independent variable) we show that the transition towards ice-free conditions is actually occuring in a very similar manner for all models. For these reasons, some quantities that do not explicitly depend on time, such as the year at which SSIE drops below a certain threshold, are likely to be constrained. In a second step, using several adequate 1979–2010 sea ice metrics, we effectively reduce the uncertainty as to when the Arctic could become nearly ice-free in summertime (between 2041 and 2060 for a high climate forcing scenario).

1 Introduction

The evolution of summer Arctic sea ice in the next decades is of particular economic, ecological and climatic relevance (ACIA, 2005). Indeed, the area of surviving Arctic sea ice at the end of the melt season (in September) determines in large part the proportion of seasonal, first-year ice in the following months. Given that the shift towards a full first-year sea ice regime would have important implications (for example, the first-year ice is thinner, more permeable and contains a higher proportion of biogeochemical contents than multi-year ice), the recent observed dramatic sea ice retreats in late summer (2005, 2007, 2008, 2011; Fetterer et al., 2012) stress the urgent need for extracting reliable information from the abundant existing projections of Arctic sea ice. Here we examine the 21st century projections of summer Arctic sea ice from 29 Earth system and general circulation models (ESMs and GCMs) participating to the Coupled Model Intercomparison Project, phase 5 (CMIP5, http://pcmdi3.llnl.gov/esgcet). All these models project a decline in summer Arctic sea ice extent over the next decades for medium and high forcing scenarios (Fig. 1).

Nonetheless, large uncertainties remain regarding the magnitude and timing of future changes in the sea ice cover. This was already underlined for CMIP3, the previous round of model intercomparison (see, e.g. Arzel et al., 2006; Zhang and Walsh, 2005), and several studies have proposed to reduce the spread in sea ice projections through model selection/weighting (Zhang and Walsh, 2005; Stroeve et al., 2007; Wang and Overland, 2009, 2012; Zhang, 2010) and/or model recalibration/extrapolation on available observations (Boé et al., 2009; Wang and Overland, 2009, 2012; Mahlstein and Knutti, 2012). Both approaches present potential drawbacks. In the former, one needs to identify a reasonable criterion for selection and, if the models are to be combined collectively, a sound multi-model weighting rule. In the latter, one has to work with the hypothesis that the recalibration is physically robust and meaningful, given that the different models are often in very different states.

To the best of our knowledge, only four studies have made use of the CMIP5 output of Arctic sea ice so far. Pavlova et al. (2011) focused on the recent model properties and showed that the 1980–1999 Arctic mean sea ice extent in CMIP5 models is closer to reality than for CMIP3, in both winter and summer. Stroeve et al. (2012) also reported that the Arctic sea ice extent properties are better reproduced with the CMIP5 models; their results suggest, in line with other recent studies (e.g. Notz and Marotzke, 2012), that the role of external forcings on the simulated and observed summer Arctic sea ice retreat is becoming increasingly clear. In a recent review, Maslowski et al.

TCD
6, 2931–2959, 2012
CMIP5 Arctic sea ice
F. Massonnet et al.

(2012) describe the recent Arctic sea ice properties simulated by 8 CMIP5 models and point out that large biases still remain compared to CMIP3 (for example, 4 of the 8 CMIP5 models considered display an unrealistic summer sea ice thickness distribution). Finally, Wang and Overland (2012) make a CMIP5 model selection based on their climatological sea ice extent properties and adjust the summer sea ice extents of these models to the observed value as to narrow the large spread present among the different integrations.

In this work, we focus on the summer Arctic sea ice projections and show that several variables related to the current 1979–2010 sea ice state are robust in constraining (i.e. influencing the future behaviour of) the most recent generation of summer Arctic sea ice projections. Both metrics characterizing the mean sea ice properties (e.g. the mean 1979–2010 September sea ice extent, the 1979–2010 annual mean volume) and the multi-decadal variability of the sea ice cover (the 1979–2010 trend in September sea ice extent) are considered. In our selection, we take into account the effects of internal variability (particularly large for the trend) as to not reject models for wrong reasons. In this paper, we also identify that the transition from stable, pre-industrial states to seasonally (near) ice-free conditions is marked by a nonlinear relationship between the local mean sea ice and the contemporary trend. This strengthens our initial idea that simulating a reasonable current sea ice state over the recent decades is a necessary condition to limit biases in summer Arctic sea ice projections.

2 Model output and observational data

Table 1 lists the 29 ESMs and GCMs used for this study, selected on the requirement that they archive sea ice fields up to 2100 (a final sample of ~35 models is expected when all simulations are uploaded onto the repository). Out of the existing climate forcing scenarios, we only retain two “representative concentration pathways” (RCPs, Moss et al., 2010): RCP4.5 and RCP8.5. The radiative forcing in RCP8.5 increases nearly steadily over the 21st century to peak at +8.5 $\mathrm{W\,m^{-2}}$ in 2100 relative to pre-industrial levels. In RCP4.5, the increase is also nearly linear up to 2060, and then eventually flattens out so that a net value of +4.5 $\mathrm{W\,m^{-2}}$ is reached in 2100 (van Vuuren et al., 2011). Because of the much smaller population of available models under RCP2.6 and RCP6.0, these two other scenarios are not discused here.

For each simulation, we derive three quantities from the monthly sea ice fields on the model native grid: the sea ice extent (calculated as the area of grid cells comprising at least 15 % of ice); the total sea ice volume (sum, over the grid cells, of the grid cell area multiplied by the mean thickness including open water), and the thin ice extent (the extent of sea ice with mean grid cell thickness between 0.01 and 0.5 m). Working on the original grid is a well-founded choice, (1) because the grid is part of the model experimental design, and (2) because no ice is artificially created/removed due to interpolation onto a common grid, with a prescribed land-sea mask. However, as the area covered by ocean in the Arctic (e.g. $>65^{\circ}$ N) is different on each model grid ($\sim$ 1.8 million $\mathrm{km^2}$ difference between the extremes), care must be taken when the output is analyzed.

Here the term "CMIP5 model" refers to each of the 29 ESMs and GCMs listed in Table 1. If a model comprises several members, then an equally-weighted average of these members is considered but the distribution of the members is still displayed. Therefore, for models with members, we use the mean of the members to evaluate the average characteristics of this model, the scatter of the ensemble providing information on the possible contribution of internal variability in additional analyses. For the other models, the information relies on the only one available realization. Finally, the term "multi-model mean" refers to the average across all CMIP5 models, with equal weight.

Observations of sea ice extent are taken from the National Snow and Ice Data Center (NSIDC) sea ice index (Fetterer et al., 2012). The data is provided as monthly values calculated on a polar stereographic 25 km resolution grid, with the same 15 % cutoff definition as that described in the previous paragraph. We perform the comparison to observations over the 1979–2010 reference period. For that purpose, we have extended the 1979–2005 available CMIP5 sea ice output from the historical simulations

TCD
6, 2931–2959, 2012

Title Page
Abstract Introduction
Conclusions References
Tables Figures
◂◂ ▸▸
◂ ▸
Back Close
Full Screen / Esc
Printer-friendly Version
Interactive Discussion

with the 2006–2010 fields under RCP4.5. At such short time scales and so early in the 21st century, the choice of the scenario to complete the 1979–2005 time series is of no particular importance (not shown).

3 Results

3.1 1979–2010 summer sea ice characteristics

A summary of the summer Arctic sea ice extent characteristics simulated by the 29 CMIP5 models and their members is shown in Fig. 2 for the 1979–2010 reference period. We make the distinction between the climatological mean state (x-axis) and the linear trend (y-axis) over that period. The multi-model mean compares well with the observed September sea ice extent (SSIE) (x-axis). The distribution of the extents among CMIP5 models is roughly symmetric about the multi-model mean, with one notable outlier (CSIRO-Mk3.6.0). The width of the distribution is substantial (~ 7 million km^2) and has not narrowed since CMIP3 (Parkinson et al., 2006).

The CMIP5 multi-model mean underestimates the observed trend (y-axis in Fig. 2). However the observations lie inside the distribution of the modeled trends (as an ensemble), and hence, the models cannot be considered inconsistent with the observed trend. The same is true for CMIP3 models for the 1979–2006 period as shown by Stroeve et al. (2007). It is worth noting that the magnitude of the SSIE trend of the multi-model mean for 1979–2006 is considerably higher in the CMIP5 models compared to CMIP3 models (not shown here), suggesting that model improvements/tuning have caused models to have greater sea ice decline in September (see also Stroeve et al., 2012, for a detailed analysis of the CMIP5 model trends in summer Arctic sea ice extent).

TCD
6, 2931–2959, 2012

3.2 21st century summer sea ice projections

All the models examined in this study project a decline in the summer sea ice extent over the present century (Fig. 1). Consistently, the response is faster for individual models and the multi-model mean under the higher emission scenario (RCP8.5). Still, the spread in the projections remains large: whether ice-free conditions (defined here as < 1 million km^2 and marked with a horizontal black line in Fig. 1) will be reached in summer by 2100 is not clear: roughly 50 % of the models are ice-free at the end of the century in RCP4.5 (in accordance with the results of Stroeve et al., 2012) and, under RCP8.5, the question is to determine when exactly the Arctic is first ice-free.

One method for addressing, understanding and possibly narrowing this spread is to study the future sea ice characteristics as a function of the present-day state. Whether or not a relationship could exist between the two time periods is not clear: with the CMIP3 data set, Arzel et al. (2006) showed that the summer mean 1981–2000 extent influences the relative (i.e. in %) but not the absolute changes in SSIE. However, this is a concern, since a relationship can be found by construction even though the mean X and the projected changes ΔX are actually independent[1]. Besides, they found no relationship between the 1981–2000 mean sea ice thickness and future SSIE changes. On the other hand, Holland et al. (2008) found that the baseline thickness of ice is well

[1]Let X be a random vector consisting of 29 elements (the number of models used in this study) sampled from a normal distribution with a mean of 8 million km^2 and a variance of 1 million km^2; let ΔX be another random vector (independent of X) of the same length in which each element is sampled from a normal distribution with a mean of -4 million km^2 and a variance of 1 million km^2. Then out of 100 000 independent draws for X and ΔX, corr(X,$\Delta X/X$) is 80.84 % of the time greater than 0.3115, the level corresponding to a p-value smaller than 5 % for classical one tail Student t-test with $29 - 2 = 27$ degrees of freedom (corr(X, ΔX) is greater than 0.3115 in 5.04 % of the cases, as expected). In a more extreme case (constant ΔX of -4 million km^2 for all models), corr(X, $\Delta X/X$) is 100 % of the time greater than 0.3115; that is, even if the projected changes ΔX are constant across the models, correlations will be artificially high and significant simply due to the use of relative values.

TCD
6, 2931–2959, 2012

correlated with the SSIE throughout the 21st century. Using the CMIP2 data set, Flato (2004) – yet using annual mean values of Arctic sea ice extent – reported that the initial extent does not strongly impact future changes in sea ice extent; this is consistent with the hypothesis that, if such relationships exist, they may be seasonally-dependent (Bitz et al., 2012). Boé et al. (2009) found that the future remaining SSIE correlates well with the 1979–2007 trends in SSIE and the area of thin (0.01–0.5 m) ice over 1950–1979, but again they worked with relative values. Moreover, the relationship involving the 1950–1979 thin ice area does not necessarily hold over the more recent (1979–2007) period. To summarize, it is not clear to date whether or not a relationship may exist between the present-day (1979–2010) sea ice cover and its projected changes. We propose below to review without ambiguity the possible existence or not of such mechanisms in the most recent generation of climate models.

With the CMIP5 data set, there is no clear and robust linear relationship between the 1979–2010 sea ice characteristics and the projected changes (anomalies) in SSIE at a given time period. As an example (left part of Table 2), across the CMIP5 models, the correlation between (1) the mean 1979–2010 SSIE (predictor I in Table 2) and (2) the SSIE change between 1979–2010 and 2030–2061 (the predictand) under RCP4.5 is 0.38 (significant at $p < 0.05$) but drops to 0.20 (non significant at $p < 0.05$) for 2069–2100. The other correlations given in the left part of Table 2 are not convincing: when they are significant, their sign (indicating the direction of the relationship) is found to be scenario and time-period dependent as illustrated when ice volume is used as a predictor. This absence of strong linear relationship makes sense: over a given time period (e.g. 2030–2061), the CMIP5 models are in highly different states (Fig. 1). Some are at (near) ice-free conditions (e.g. MIROC-ESM, MIROC-ESM-CHEM, GFDL-CM3) and thus in a stationary state, while some others are at near present-day levels and still on the track of ice loss (e.g. CSIRO-Mk6.3.0, NorESM1-M, FGOALS-G2).

To account for the fact that the CMIP5 model population has diverse characteristics at any particular time, we propose to analyze the present-future relationships from a slightly different perspective. Let Y_i be the year after 1979 where the CMIP5 model

TCD
6, 2931–2959, 2012

i reaches a given SSIE (for example, 4 million km^2) for the first time. The Y_i's (predictands) correlate better and with more consistency (i.e. the direction of the relationships does not change) to the different predictors listed in Table 2 (right part). For example, across the CMIP5 models, the year at which the SSIE drops below 4 million km^2 under RCP4.5 correlates significantly ($p < 0.001$) at 0.72 with the 1979–2010 mean annual volume. The right part of Table 2 supports evidence that all the five criteria listed in the table (predictors) are potential candidates for applying a constraint on the available CMIP5 models and, by doing so, potentially reducing the large scatter in SSIE projections; the left part of the table suggests that the relationships invoked for applying such constraints are not necessarily straightforward, at least in a linear framework.

Out of the 5 predictors listed in Table 2, two of them deserve particular attention: the 1979–2010 mean SSIE (I) and the 1979–2010 trend in SSIE (V). Indeed, as shown in the previous paragraph, the time taken for the SSIE to reach a given extent is, on the one hand, well correlated with the summer initial extent. This occurs because the CMIP5 simulations have nearly the same long-term trend in SSIE as they approach ice-free conditions. As an example, under RCP8.5, the SSIE trends from 1979 up to the year when ice-free (1 million km^2) conditions are reached is $-772 \pm 165 \times 10^3$ km^2 decade^{-1} (mean of the CMIP5 $\pm$ 1 std). On the other hand, the trends are weaker and more scattered over the 1979–2010 period as discussed in section 3.1 and shown in Fig. 2 ($-560 \pm 298 \times 10^3$ km^2 decade^{-1}).

The trends are more uniform over the longer period because the transition between the two main stationary states for each model (pre-industrial and ice-free conditions) is marked by a rapid loss of SSIE at some point in most 21st century integrations, as also found in some of the CMIP3 models (Holland et al., 2006). These rapid ice loss periods are the dominate cause of ice loss over the longer period. Such an event occurs in all CMIP5 models when they approach ice-free conditions and manifests as a marked minimum of the running trend during the 21st century (identified with the RCP8.5 simulation in Fig. 3). The timing of the minimum trend (marked with a vertical bar in Fig. 3) varies between 2000 and 2100 in the CMIP5 ensemble. For this reason, it cannot result from a sudden acceleration of the prescribed radiative forcing since the individual events do not happen simultaneously among integrations. This is another indication, confirming the results of Table 2, that the 21st century CMIP5 model summer sea ice characteristics are not expected to be similar over common time periods.

Let us instead consider the mean SSIE as the independent coordinate for describing the trend evolution. In Fig. 4, we show the trajectories of SSIE in a phase space diagram (SSIE against its time derivative, i.e. its trend) in the case of RCP8.5. In these plots (in which the time is thus an implicit variable), clear similarities come to light. All models follow a similar trajectory: they start from the right (relatively high mean SSIE at the beginning of the simulation), then move leftwards as the mean SSIE decreases. Then, they all experience a U-shaped trajectory as the mean SSIE decreases further to ice-free conditions (the 2030–2061 position of each model is marked with a colored dot). In Fig. 2, the spread in the CMIP5 population is thus represented by the different 1979–2010 positions of the CMIP5 models on their trajectories (colored crosses): for example, BCC-CSM1.1, CanESM2 and GISS-E2-R are already near the minimum, while EC-EARTH and CCSM4 have not reached it yet. Under RCP4.5, similar trajectories exist (Fig. S1) for the subset of models that reach ice-free conditions in September by $\sim$2060 – the approximate year at which the RCP4.5 forcing stabilizes – suggesting that, as long as the SSIE reaches (near) ice-free conditions under the effect of increased radiative forcing, the U-shaped trajectory occurs.

4 Discussion

It is well known that the reduction in summer and annual Arctic sea ice cover is tightly linked to increased greenhouse gas forcing/global warming (e.g. Gregory et al., 2002; Flato, 2004; Ridley et al., 2007; Zhang, 2010; Winton, 2011; Mahlstein and Knutti, 2012). However, while the climate forcing acts as a clear driver for summer sea ice retreat, the internal dynamics of the system still appears to play an important role if the Arctic basin approaches ice-free conditions. The evolution of the projected summer

TCD
6, 2931–2959, 2012

Arctic sea ice extent is indeed marked by an elevated rate of decline, much greater than ever before (i.e. a visible minimum in its running trend, Fig. 4), this event being clearly model-dependent in the time domain (vertical bars in Fig. 3) but not in the SSIE domain (it occurs at ~2–4 million km^2, Fig. 4). In a previous study, Goosse et al. (2009) showed that the variance in detrended SSIE is also dependent on the mean SSIE in the Arctic for various climate models, with a peak at comparable SSIE (between 2 and 4 million km^2). In our case, the elevated rates of summer sea ice decline probably stem from the fact that (1) wider areas of open ocean surround the summer sea ice cover when it reaches lower extents, making the ice more vulnerable to oceanic heat fluxes than if the Arctic basin was (almost) saturated with ice, and (2) the ice gets thinner in the course of the 21st century, and open water forms at higher rates in this case (Holland et al., 2006). When ice-free conditions are eventually reached, there is by definition no interannual variability (the (0, 0) coordinates in Fig. 4). This boundary condition in the phase space gives the trajectories their full U-shaped appearance.

Altogether, Table 2 and Fig. 4 summarize why linking present-day sea ice conditions (predictors) to projected SSIE anomalies (predictand) in the time domain is not straightforward. In Fig. 4, the SSIE loss between 1979–2010 and 2030–2061 is graphically represented by the x-distance between the colored cross and the colored dot in each panel. The SSIE loss is small for models with extensive ice (e.g. CSIRO-Mk3.6.0, NorESM1-M, FGOALS-g2) because the trends in SSIE do not reach low values when the mean SSIE is high. The SSIE loss is larger for models with medium 1979–2010 SSIE (e.g. GFDL-CM3, MIROC-ESM, MIROC-ESM-CHEM) because these models start at the right edge of the U trajectories and the trends are becoming increasingly greater over time. Finally, the SSIE loss is smaller for models with initial small SSIE (e.g. CanESM2, GISS-E2-R, BCC-CSM1.1): they start in the lowest part of the U and the magnitude of the trends in SSIE are thus becoming smaller over time. The nonlinearity of the trends identified in Fig. 4 makes therefore the correlations in the left part of Table 2 weak, with opposite signs and often non significant in the course of the 21st century.

TCD
6, 2931–2959, 2012

Nonetheless, a clear relationship exists if the predictand is modified so that the SSIE is chosen as the independent coordinate (right part of Table 2). Our analysis suggests that CMIP5 models tend to reach a given summer sea ice extent earlier when (i) the amplitude of their climatological cycle of sea ice extent is larger, (ii) the extent of thin (< 0.5 m) ice is larger in September, (iii) they have thinner ice in the annual mean, (iv) they have smaller initial September sea ice extent, and (v) they lose ice at higher rates now. These results can be interpreted in light of simple physical mechanisms, resp. (i) the seasonal cycle of sea ice extent is a proxy for the model sensitivity to external forcings, (ii) the ice is more susceptible to melt away in areas where it is thin, (iii) and (iv) models with a larger initial volume of ice need more energy, and thus time, to melt ice and reach a given extent, and (v) the most sensitive models now are likely to reach ice-free conditions earlier under future warming. It is also important to stress that these criteria are not fully independent (e.g. the amplitude of the 1979–2010 mean seasonal cycle of sea ice extent correlates significantly ($p < 0.001$) at 0.67 with the 1979–2010 mean September thin ice extent in the CMIP5 models).

It remains yet to determine how the five criteria listed in Table 2 can be used in practice for model selection, given that the 1979–2010 period used for evaluation is short (32 yr time period) and that the effects of internal variability on statistics of time series are then potentially high. The different members of the CMIP5 models are supposed to sample, at least in part, the uncertainty associated with this internal variability by slightly perturbing initial conditions/sensitive parameters. While the effects on the mean 1979–2010 SSIE are moderate (Fig. 2, see how the dots of the same color cluster in the x-direction), the 1979–2010 trends in SSIE are clearly different from member to member (same figure, see how the dots of the same color scatter in the y-direction).

In order to be more quantitative, an evaluation of the effects of internal variability for criteria I and V is given in Fig. 5 as a function of the time period length used for calculation. The effects of internal variability on the trend in SSIE (left panel) and on the mean SSIE (right panel) are measured by (1) considering the different available members of the CMIP5 models and (2) by slightly changing the end points of the time periods. With

~ 30 yr of data, the relative spread is considerable for the trends (more than 100 % for some models) but decreases when longer time periods are used; it is smaller (less than 20 %) for the mean and not decreasing if a longer time period is considered. For these reasons, a metric based on the 1979–2010 SSIE trend must certainly account for these effects, given that (1) only one observed climate realization is available, recorded on (2) a very short time period, and (3) the number of members for the CMIP5 models (see Table 1) is quite small to properly sample the distribution of possible trends. Note that the scatter in Fig. 5a is larger for models with members, indicating that the trends are the most sensitive to changes in physical parameters/initial conditions than to the end points used for calculation. Presented the other way around, the trends in SSIE derived from models with one single member but with different end points sample only a limited region of their full possible trends distribution. This limitation needs to be taken into account in the analysis.

Accordingly, we propose the following practical rule for model selection. Let C be one of the metrics of Table 2 (i.e. one of the predictors). For multi-member models, we require that at least one member of the model lies within 20 % of the observations (the numerical value of 20 % is arbitrary, but identical to that of Stroeve et al., 2007; Wang and Overland, 2009, 2012). In other words, for a model i with several members, the 20 % interval around the observations needs to overlap I_i, the interval between the two extreme members of i. The average range $\overline{r}$ obtained from these multi-member models (i.e. the average length of the I_i's) is then used for assessing the performance of models with only one member (for which we do not have the information about the contribution of internal variability on the simulated value of C): for these single-member models, we require that the simulated value of metric $C \pm \overline{r}$ overlaps the ± 20 % interval around the observations. That is, all models are evaluated by taking the effects of internal variability into account either directly for multi-member models (with the information from the model's own members), or indirectly for the single-member models (considering the average contribution of internal variability obtained from the multi-member models).

TCD
6, 2931–2959, 2012
CMIP5 Arctic sea ice
F. Massonnet et al.

We retain first the models with a reasonable sea ice extent, i.e. we only select models that simulate the SSIE and amplitude of the sea ice extent seasonal cycle reasonably. 13 CMIP5 models (ACCESS1.0, ACCESS1.3, CCSM4, EC-EARTH, GFDL-CM3, HadGEM2-CC, INM-CM4, IPSL-CM5A-LR, IPSL-CM5A-MR, MIROC-ESM, MIROC-ESM-CHEM, MPI-ESM-LR and MPI-ESM-MR) satisfy the requirements. Considering only these 13 models, the 5-yr smoothed SSIE drops below 1 million km^2 for at least 5 consecutive years between 2029 (earliest model) and 2076 (latest model) for RCP8.5 (between 2029 and sometime after 2100 without the constraint, i.e. if all CMIP5 models are considered), and between 2032 and sometime after 2100 for RCP4.5 (same without the constraint).

Now we note that, out of this subset of 13 models, the models dropping below 1 million km^2 earlier (later) in the 21st century are also thinner (thicker) in the annual mean over 1979–2010 (not shown here, but in accordance with Table 2, right part). This suggests that a further model selection through ice volume assessment can be applied. Since no long-term and spatially homogenous data of sea ice thickness is available from observations, we take as our best estimate the 1979–2010 annual mean sea ice volume from the PIOMAS sea ice reanalysis (Schweiger et al., 2011). Although this reanalysis is an extremely valuable tool, one has to bear in mind that the sea ice volume is obtained from a model constrained by sea ice concentration and sea surface temperature data assimilation, and the ice thickness (and hence volume) is likely to be biased. For this reason, an adjusted estimate of the volume based on in-situ observations of sea ice thickness (method described in Schweiger et al., 2011) is used (A. Schweiger, personal communication, 2012). Retaining the CMIP5 models lying within 20 % of the adjusted PIOMAS 1979–2010 annual mean sea ice volume of $18.95 \times 10^3\,km^3$, we keep 9 models (the 13 minus CCSM4, EC-EARTH, MIROC-ESM and MIROC-ESM-CHEM). Considering now these 9 models only, the 5-yr smoothed SSIE drops below 1 million km^2 for 5 consecutive years between 2041 and 2069 for RCP8.5, and between 2040 and sometime after 2100 for RCP4.5.

TCD
6, 2931–2959, 2012

For finally refining the selection, we only consider models with a reasonable trend in SSIE over 1979–2010. We end up with 6 models (ACCESS1.0, ACCESS1.3, GFDL-CM3, HadGEM2-CC, IPSL-CM5A-MR, MPI-ESM-MR). With these 6 models only, the 5-yr smoothed SSIE drops below 1 million km^2 for 5 consecutive years between 2041 and 2060 for RCP8.5, and between 2040 and sometime after 2100 for RCP4.5. Very interestingly, exactly the same 6 models are retained if the same selection procedure is conducted over 1979–2006, suggesting that our evaluation is robust in practice. Note that the time interval for summer Arctic sea ice disappearance under RCP8.5 obtained in this study (2041–2060) is different from that obtained by Wang and Overland (2012) using selection and recalibration of the CMIP5 models (2021–2043). However, a re-calibration is a debatable approach for constraining the summer Arctic sea ice extent, given that the trends (and thus the anomalies in sea ice extent) are locally dependent on the current mean sea ice extent (Fig. 4).

As a final comment, we would like to discuss another possible option aimed at reducing the spread in summer Arctic sea ice projections. Instead of applying a model selection, one could consider to retain a linear combination of the models (e.g. the multi-model mean, or a weighted average of the different models). The multi-model mean is actually a good candidate (excellent mean 1979–2010 SSIE, Fig. 2). As long as the CMIP5 models are not at (near) ice-free conditions, the CMIP5 model distribution is approximately Gaussian and symmetric (e.g. Fig. 2), two important properties that make the multi-model mean an informative variable. However, because the system is characterized by a highly nonlinear behaviour at low SSIE, and because the SSIE is by definition bounded by 0, the CMIP5 model distribution loses these two important properties when low SSIEs are reached. Consequently, the multi-model mean is no longer a good representative of the distribution since it results from an average of models in highly different states. A good illustration is given in Fig. 3: the U-shape present in each individual model is much more flat and less intense in the multi-model mean, simply because it results from an average of all models at identical times; in other words, the diverse behaviours in each individual CMIP5 model are much less visible in the multi-model mean.

5 Conclusions

The 21st century projections of summer Arctic sea ice are now available from the most recent effort of coupled model inter-model comparison, CMIP5. Here we consider 29 models available to date (we started from the principle that none of the available CMIP5 models should be dismissed prior to the analysis, e.g. Arzel et al., 2006). Noticing a considerable spread in the summer sea ice simulations over the 21st century, we raise the question of model selection as an opportunity to reduce these uncertainties. In a first step, we find that the CMIP5 models projected anomalies of September sea ice extent (SSIE) (with respect to their own 1979–2010 climatology) are linked in a complicated manner to the 1979–2010 characteristics of their sea ice cover, owing to an acceleration of the trends (and thus larger anomalies) in SSIE, which occurs at different times during the 21st century, but at a mean SSIE of $\sim$2–4 million km^2. Nonetheless, other predictands that do not depend explicitly on the time (e.g. the year at which SSIE drops below a certain value) correlate well with the 1979–2010 sea ice properties and support the idea that a reduction of spread through model selection is possible.

In a second step, we examine the different common sea ice variables used for assessment and discuss their practical suitability for model selection. Over 1979–2010 (a relatively short time period for climate studies), the effects of internal variability can be pronounced (see, e.g. Fig. 5) and care must be taken when assessing a model performance over this period. In this work, we tried to account for these effects and showed that it is possible to actually constrain the date of disappearance of Arctic summer sea ice, based on the models baseline 1979–2010 mean sea ice extent and volume properties, but also on the response of these models to external forcings (evaluated here with the trend in SSIE). Although the choice of the reference product for sea ice volume is debatable (we use a reanalysis), it shows at least that a selection based on the volume effectively contributes to reduce the uncertainties. The 1979–2010 mean September thin ice extent would be another information useful for constraining the projections, and could be indirectly used from observations of the sea ice age (Maslanik et al., 2007). Note that a further perspective in constraining the projections would be to assess the models on their dynamical properties (e.g. the sea ice drift or the export of ice through Fram Strait), also potentially important for the future global sea ice mass balance (Rampal et al., 2011). Unfortunately, a limited number of models (about 50 % of the 29 CMIP5 models) archive sea ice velocity. Besides, defining adequate criteria for evaluation is challenging given that the sea ice dynamics operate on a very large spectrum both in the time and spatial domains (Rampal et al., 2009).

Our results are valid in the context of climate projections at the century time scale, and an equivalent inter-model study at shorter time scales, assessing for example the potential of ocean-sea ice initialization onto the simulated SSIE variability, is still lacking (to the best of our knowledge). We have shown that it is possible to constrain the date of possible disappearance of summer Arctic sea ice as simulated by the CMIP5 models (this date depending also on the forcing scenario that is considered) on this basis. The retention of 6 CMIP5 models based on their 1979–2010 sea ice extent and volume characteristics reduces the uncertainty as to when the Arctic could become ice-free in summer from $[2029, 2100^+]$ to $[2041, 2060]$ for the high forcing scenario RCP8.5 ($2100^+ =$ sometime after 2100). For the medium forcing scenario RCP4.5, the uncertainty in the year of summer Arctic sea ice disappearance reduces from $[2032, 2100^+]$ to $[2040, 2100^+]$. The narrowing is not as clear as with the high forcing scenario, and suggests that the sea ice cover is also sensitive to other factors, e.g. the near-surface global or Arctic air temperature (Mahlstein and Knutti, 2012; Zhang, 2010) or the meridional oceanic heat flux (Mahlstein and Knutti, 2011). Our study therefore indicates that simulating a correct sea ice state over 1979–2010 is a necessary condition to reasonably anticipate future sea ice evolution, as it has a clear influence on the variability and response of the sea ice cover.

TCD
6, 2931–2959, 2012

Supplementary material related to this article is available online at: http://www.the-cryosphere-discuss.net/6/2931/2012/tcd-6-2931-2012-supplement.zip.

Acknowledgements. We acknowledge the World Climate Research Programme's Working Group on Coupled Modelling, which is responsible for CMIP, and we thank the climate modeling groups (listed in the Supplement) for producing and making available their model output. For CMIP the US Department of Energy's Program for Climate Model Diagnosis and Intercomparison provides coordinating support and led development of software infrastructure in partnership with the Global Organization for Earth System Science Portals. We thank P. Mathiot and M. Vancoppenolle for their helpful comments. FM is a F.R.S.-FNRS Research Fellow. HG is a F.R.S.-FNRS Senior Research Associate. This work was partly funded by the European Commission's 7th Framework Programme, under Grant Agreement number 226520, COMBINE project (Comprehensive Modelling of the Earth System for Better Climate Prediction and Projection). It was also partly supported by the Belgian Science Federal Policy Office (BELSPO) and by the US Office of Naval Research through grant N00014-11-1-0550 (CMB).

References

ACIA, Arctic Climate Impact Assessment (ACIA): Scientific Report, Cambridge University Press, Fairbanks, 2005. 2932

Arzel, O., Fichefet, T., and Goosse, H.: Sea ice evolution over the 20th and 21st centuries as simulated by current AOGCMs, Ocean Model., 12, 401–415, 2006. 2933, 2937, 2946

Bitz, C. M., Ridley, J., Holland, M., and Cattle, H.: Global climate models and 20th and 21st century Arctic climate change, in: Arctic Climate Change: The ACSYS Decade and Beyond, chapter 11, edited by: Lemke, P. and Jacobi, H. W., Springer, Dordrecht and New York, 2012. 2938

Boé, J., Hall, A., and Qu, X.: September sea-ice cover in the Arctic Ocean projected to vanish by 2100, Nat. Geosci., 2, 341–343, 2009. 2933, 2938

Fetterer, F., Knowles, K., Meier, W., and Savoie, M.: Sea ice index, Electronic, available at: http://nsidc.org/data/seaice_index/ (last access: July 2012), 2012. 2933, 2935, 2955, 2956

Flato, G. M.: Sea-ice and its response to CO_2 forcing as simulated by global climate models, Clim. Dynam., 23, 229–241, 2004. 2938, 2940

Gent, P. R., Danabasoglu, G., Donner, L. J., Holland, M. M., Hunke, E. C., Jayne, S. R., Lawrence, D. M., Neale, R. B., Rasch, P. J., Vertenstein, M., Worley, P. H., Yang, Z.-L., and Zhang, M.: The Community Climate System Model Version 4, J. Climate, 24, 4973–4991, doi:10.1175/2011JCLI4083.1, 2011. 2953

Goosse, H., Arzel, O., Bitz, C. M., de Montety, A., and Vancoppenolle, M.: Increased variability of the Arctic summer ice extent in a warmer climate, Geophys. Res. Lett., L23702, doi:10.1029/2009GL040546, 2009. 2941

Gregory, J. M., Stott,. P. A., Cresswell, D. J., Rayner, N. A., Gordon, C., and Sexton, D. M. H.: Recent and future changes in Arctic sea ice simulated by the HadCM3 AOGCM, Geophys. Res. Lett., 29, 2175, doi:10.1029/2001GL014575, 2002. 2940

Griffies, S. M., Winton, M., Donner, L. J., Horowitz, L. W., Downes, S. M., Farneti, R., Gnanadesikan, A., Hurlin, W. J., Lee, H.-C., Liang, Z., Palter, J. B., Samuels, B. L., Wittenberg, A. T., Wyman, B. L., Yin, J., and Zadeh, N.: The GFDL CM3 Coupled Climate Model: Characteristics of the Ocean and Sea Ice Simulations, J. Climate, 24, 3520–3544, http://dx.doi.org/10.1175/2011JCLI3964.1, 2011. 2953

Hazeleger, W., Severijns, C., Semmler, T., Stefanescu, S., Yang, S., Wang, X., Wyser, K., Dutra, E., Baldasano, J. M., Bintanja, R., Bougeault, P., Caballero, R., Ekman, A. M. L., Christensen, J. H., van den Hurk, B., Jimenez, P., Jones, C., Kallberg, P., Koenigk, T., McGrath, R., Miranda, P., Van Noije, T., Palmer, T., Parodi, J. A., Schmith, T., Selten, F., Storelvmo, T., Sterl, A., Tapamo, H., Vancoppenolle, M., Viterbo, P., and Willén, U.: EC-Earth: A Seamless Earth-System Prediction Approach in Action, B. Am. Meteorol. Soc., 91, 1357–1363, doi:10.1175/2010BAMS2877.1, http://journals.ametsoc.org/doi/abs/10.1175/2010BAMS2877.1, 2010. 2953

Holland, M. M., Bitz, C. M., and Tremblay, B.: Future abrupt reductions in the summer Arctic sea ice, Geophys. Res. Lett., 33, L23503, doi:10.1029/2006GL028024, 2006. 2939, 2941

Holland, M., Serreze, M. M., and Stroeve, J.: The sea ice mass budget of the Arctic and its future change as simulated by coupled climate models, Clim. Dynam., 34, 185–200, 2008. 2937

Johns, T. C., Durman, C. F., Banks, H. T., Roberts, M. J., McLaren, A. J., Ridley, J. K., Senior, C. A., Williams, K. D., Jones, A., Rickard, G. J., Cusack, S., Ingram, W. J., Crucifix, M., Sexton, D. M. H., Joshi, M. M., Dong, B.-W., Spencer, H., Hill, R. S. R., Gregory, J. M., Keen,

A. B., Pardaens, A. K., Lowe, J. A., Bodas-Salcedo, A., Stark, S., and Searl, Y.: The New Hadley Centre Climate Model (HadGEM1): Evaluation of Coupled Simulations, J. Climate, 19, 1327–1353, http://dx.doi.org/10.1175/JCLI3712.1, 2006. 2953

Jungclaus, J. H., Keenlyside, N., Botzet, M., Haak, H., Luo, J.-J., Latif, M., Marotzke, J., Mikolajewicz, U., and Roeckner, E.: Ocean Circulation and Tropical Variability in the Coupled Model ECHAM5/MPI-OM, J. Climate, 19, 3952–3972, http://dx.doi.org/10.1175/JCLI3827.1, 2006. 2953

Mahlstein, I., and Knutti, R.: Ocean heat transport as a cause for model uncertainty in projected arctic warming, J. Climate, 24, 1451–1460, 2011. 2947

Mahlstein, I., and Knutti, R.: September Arctic sea ice predicted to disappear for 2 °C global warming above present, J. Geophys. Res., 117, D06104, doi:10.1029/2011JD016709, 2012. 2933, 2940, 2947

The HadGEM2 Development Team: Martin, G. M., Bellouin, N., Collins, W. J., Culverwell, I. D., Halloran, P. R., Hardiman, S. C., Hinton, T. J., Jones, C. D., McDonald, R. E., McLaren, A. J., O'Connor, F. M., Roberts, M. J., Rodriguez, J. M., Woodward, S., Best, M. J., Brooks, M. E., Brown, A. R., Butchart, N., Dearden, C., Derbyshire, S. H., Dharssi, I., Doutriaux-Boucher, M., Edwards, J. M., Falloon, P. D., Gedney, N., Gray, L. J., Hewitt, H. T., Hobson, M., Huddleston, M. R., Hughes, J., Ineson, S., Ingram, W. J., James, P. M., Johns, T. C., Johnson, C. E., Jones, A., Jones, C. P., Joshi, M. M., Keen, A. B., Liddicoat, S., Lock, A. P., Maidens, A. V., Manners, J. C., Milton, S. F., Rae, J. G. L., Ridley, J. K., Sellar, A., Senior, C. A., Totterdell, I. J., Verhoef, A., Vidale, P. L., and Wiltshire, A.: The HadGEM2 family of Met Office Unified Model climate configurations, Geosci. Model Dev., 4, 723–757, doi:10.5194/gmd-4-723-2011, 2011. 2953

Maslanik, J. A., Fowler, C., Stroeve, J., Drobot, S., Zwally, J., Yi, D., and Emery, W.: A younger, thinner Arctic ice cover: increased potential for rapid, extensive sea-ice loss, Geophys. Res. Lett., 34, L24501, doi:10.1029/2007GL032043, 2007. 2947

Maslowski, W., Kinney, J. C., Higgins, M., and Roberts, A.: The future of arctic sea ice, Annu. Rev. Earth Pl. Sc., 40, 625–654, 2012. 2933

Moss, R. H., Edmonds, J. A., Hibbard, K. A., Manning, M. R., Rose, S. K., van Vuuren, D. P., Carter, T. R., Emori, S., Kainuma, M., Kram, T., Meehl, G. A., Mitchell, J. F. B., Nakicenovic, N., Riahi, K., Smith, S. J., Stouffer, R. J., Thomson, A. M., Weyant, J. P., and Wilbanks, T. J.: The next generation of scenarios for climate change research and assessment, Nature, 463, 747–756, doi:10.1038/nature08823, 2010. 2934, 2955

Notz, D. and Marotzke, J.: Observations reveal external driver for arctic sea-ice retreat, Geophys. Res. Lett., 39, L08502, doi:10.1029/2012GL051094, 2012. 2933
Parkinson, C. L., Vinnikov, K. Y., and Cavalieri, D. J.: Evaluation of the simulation of the annual cycle of Arctic and Antarctic sea ice coverages by 11 major global climate models, J. Geophys. Res., 111, C07012, doi:10.1029/2005JC003408, 2006. 2936
Pavlova, T., Kattsov, V., and Govorkova, V.: Sea ice in CMIP5 models: closer to reality?, Proc. MGO, 564, 7–18, 2011 (in Russian). 2933
Rampal, P., Weiss, J., Marsan, D., and Bourgoin, M.: Arctic sea ice velocity field: general circulation and turbulent-like fluctuations, J. Geophys. Res., 114, C10014, doi:10.1029/2008JC005227, 2009. 2947
Rampal, P., Weiss, J., Dubois, C., and Campin, J.-M.: IPCC climate models do not capture Arctic sea ice drift acceleration: consequences in terms of projected sea ice thinning and decline, J. Geophys. Res., 116, C00D07, doi:10.1029/2011JC007110, 2011. 2947
Ridley, J., Lowe, J., Brierley, C., and Harris, G.: Uncertainty in the sensitivity of arctic sea ice to global warming in a perturbed parameter climate model ensemble, Geophys. Res. Lett., 34, L19704, doi:10.1029/2007GL031209, 2007. 2940
Rotstayn, L. D., Jeffrey, S. J., Collier, M. A., Dravitzki, S. M., Hirst, A. C., Syktus, J. I., and Wong, K. K.: Aerosol- and greenhouse gas-induced changes in summer rainfall and circulation in the Australasian region: a study using single-forcing climate simulations, Atmos. Chem. Phys., 12, 6377–6404, http://www.atmos-chem-phys.net/12/6377/2012/, 2012. 2953
Schweiger, A., Lindsay, R., Zhang, J., Steele, M., Stern, H., and Kwok, R.: Uncertainty in modeled arctic sea ice volume, J. Geophys. Res., 116, C00D06, doi:10.1029/2011JC007084, 2011. 2944
Stroeve, J., Holland, M. M., Meier, W., Scambos, T., and Serreze, M.: Arctic sea ice decline: faster than forecast, Geophys. Res. Lett., 34, L09501, doi:10.1029/2007GL029703, 2007. 2933, 2936, 2943
Stroeve, J., Kattsov, V., Barrett, A. P., Serreze, M., Pavlova, T., Holland, M., and Meier, W.: Trends in arctic sea ice extent from CMIP5, CMIP3 and observations, Geophys. Res. Lett., accepted, 2012. 2933, 2936, 2937
van Vuuren, D. P., Edmonds, J., Kainuma, M., Riahi, K., Thomson, A., Hibbard, K., Hurtt, G. C., Kram, T., Krey, V., Lamarque, J.-F., Masui, T., Meinshausen, M., Nakicenovic, N., Smith, S. J., and Rose, S. K.: The representative concentration pathways: an overview, Climatic Change, 109, 5–31, 2011. 2935

Voldoire, A., Sanchez-Gomez, E., Salas y Mélia, D., Decharme, B., Cassou, C., Sénési, S., Valcke, S., Beau, I., Alias, A., Chevallier, M., Déqué, M., Deshayes, J., Douville, H., Fernandez, E., Madec, G., Maisonnave, E., Moine, M.-P., Planton, S., Saint-Martin, D., Szopa, S., Tyteca, S., Alkama, R., Belamari, S., Braun, A., Coquart, L., and Chauvin, F.: The CNRM-CM5.1 global climate model: description and basic evaluation, Clim. Dynam. 1–31, doi:10.1007/s00382-011-1259-y, 2012. 2953

Volodin, Dianskii, N. A. and Gusev, A. V.: Simulating Present-Day Climate with the INMCM4.0 Coupled Model of the Atmospheric and Oceanic General Circulations, Atmos. Ocean. Phys., 46, 414–431, doi:10.1134/S000143381004002X, 2010. 2953

Wang M. and Overland, J. E.: A sea ice free summer Arctic within 30 years?, Geophys. Res. Lett., 36, L07502, doi:10.1029/2009GL037820, 2009. 2933, 2943

Wang, M. and Overland, J. E.: Summer arctic sea ice will be gone sooner or later – an update from CMIP5 models, Geophys. Res. Lett., accepted, 2012. 2933, 2934, 2943, 2945

Watanabe, M., Suzuki, T., O'ishi, R., Komuro, Y., Watanabe, S., Emori, S., Takemura, T., Chikira, M., Ogura, T., Sekiguchi, M., Takata, K., Yamazaki, D., Yokohata, T., Nozawa, T., Hasumi, H., Tatebe, H., and Kimoto, M.: Improved Climate Simulation by MIROC5: Mean States, Variability, and Climate Sensitivity, J. Climate, 23, 6312–6335, http://dx.doi.org/10.1175/2010JCLI3679.1, 2010. 2953

Watanabe, S., Hajima, T., Sudo, K., Nagashima, T., Takemura, T., Okajima, H., Nozawa, T., Kawase, H., Abe, M., Yokohata, T., Ise, T., Sato, H., Kato, E., Takata, K., Emori, S., and Kawamiya, M.: MIROC-ESM 2010: model description and basic results of CMIP5-20c3m experiments, Geosci. Model Dev., 4, 845–872, doi:10.5194/gmd-4-845-2011, 2011. 2953

Winton, M.: Do climate models underestimate the sensitivity of Northern Hemisphere sea ice cover?, J. Climate, 24, 3924–3934, doi:10.1175/2011JCLI4146.1, 2011. 2940

Zhang, X.: Sensitivity of Arctic summer sea ice coverage to global warming forcing: toward reducing uncertainty in Arctic climate change projections, Tellus A, 62, 220–227, 2010. 2933, 2940, 2947

Zhang, X. and Walsh, J. E.: Toward a seasonally ice-covered Arctic ocean: scenarios from the IPCC AR4 model simulations, J. Climate, 19, 1730–1747, 2005. 2933

Table 1. The 29 CMIP5 models used in the study, and the principal characteristics of their sea ice components.

Model	Institution	Sea Ice Component: Model	Sea Ice Component: Spatial Resolution	Sea Ice Component: Brief contents	Number of members: Hist – RCP4.5	Number of members: Hist – RCP8.5	References
ACCESS1.0	CSIRO and BOM	CICE, v4.1	tripolar, 1° × 1°, refinement at equator	Energy-conserving thermo, Ice Thickness Distribution (ITD), Elastic-Viscous-Plastic (EVP) rheology	1	1	http://wiki.csiro.au/confluence/display/ACCESS/ACCESS+Publications
ACCESS1.3	CSIRO and BOM	CICE, v4.1	tripolar, 1° × 1°, refinement at equator	Energy-conserving thermo, ITD, EVP	1	1	http://wiki.csiro.au/confluence/display/ACCESS/ACCESS+Publications
BCC-CSM1-1	BCC	SIS	tripolar,1° × (1–1/3)°	Modified Semtner 3-layer; EVP rheology; ITD	1	1	http://www.lasg.ac.cn/C20C/UserFiles/File/C20C-xin.pdf
CanESM2	CCCma	CanSIM1	T63 Gaussian Grid	Cavitating fluid	5	5	http://www.cccma.ec.gc.ca/models
CCSM4	NCAR	CICE, v4	1° orthogonal rotated, displaced pole	Energy-conserving thermo, ITD, EVP	5	6	Gent et al. (2011)
CNRM-CM5	CNRM	GELATO v5	ORCA-1°	EVP, ITD	1	5	Voldoire et al. (2012)
CSIRO-Mk6.3.0	CSIRO				10	10	Rotstayn et al. (2012)
EC-EARTH	EC-Earth consortium	LIM2	ORCA-1°	Semtner 3 layer + brine pockets, virtual ITD, Viscous-Plastic (VP) rheology	1	1	Hazeleger et al. (2010)
FGOALS-g2	IAP-THU	CICE, v4	∼ 1 × 1°	Energy-conserving thermo, ITD, EVP	1	1	http://www.lasg.ac.cn/FGOALS/CMIP5
FGOALS-s2	IAP-THU				3	3	http://www.lasg.ac.cn/FGOALS/CMIP5
GFDL-CM3	NOAA GFDL	SISp2	Tripolar grid ∼ 1° × 1°	modified Semtner 3-layer, ITD, EVP	1	1	Griffies et al. (2011)
GFDL-ESM2G	NOAA GFDL	SISp2	Tripolar grid ∼ 1° × 1°	modified Semtner 3-layer, ITD, EVP	1	1	http://nomads.gfdl.noaa.gov/
GFDL-ESM2M	NOAA GFDL	SISp2	Tripolar grid ∼ 1° × 1°	modified Semtner 3-layer, ITD, EVP	1	1	http://nomads.gfdl.noaa.gov/
GISS-E2-R	NASA GISS	Russell	1° × 1.25°		5	1	http://data.giss.nasa.gov/modelE/ar5/
HadGEM2-AO	NIMR/KMA	sea ice component of HadGOM2	1° × 1°	Semtner zero layer, ITD, EVP	1	1	Johns et al. (2006)
HadGEM2-CC	MOHC	inspired from CICE		Semtner zero layer, ITD, EVP	1	1	Martin et al. (2011)
HadGEM2-ES	MOHC				1	1	Martin et al. (2011)
INM-CM4	INM	INM-CM4	1° × 0,5°	VP	1	1	Volodin and Gusev (2010)
IPSL-CM5A-LR	IPSL	LIM2	ORCA-2°	Semtner 3 layer + brine pockets, virtual ITD, VP	3	3	http://icmc.ipsl.fr/
IPSL-CM5A-MR	IPSL	LIM2	ORCA-2°	Semtner 3 layer + brine pockets, virtual ITD, VP	1	1	http://icmc.ipsl.fr/
IPSL-CM5B-LR	IPSL	LIM2	ORCA-2°	Semtner 3 layer + brine pockets, virtual ITD, VP	1	1	http://icmc.ipsl.fr/
MIROC5	AORI-NIES-JAMSTEC	component of COCO v4.5	1.4° × (0.5°–1.4°)		1	1	Watanabe et al. (2010)
MIROC-ESM	AORI-NIES-JAMSTEC	component of COCO3.4	∼ 1,4° × 1°, L44	EVP, Semtner zero layer, 2 ice categories	1	1	Watanabe et al. (2011)
MIROC-ESM-CHEM	AORI-NIES-JAMSTEC	component of COCO3.4	∼ 1,4° × 1°, L44	EVP, Semtner zero layer, 2 ice categories	1	1	Watanabe et al. (2011)
MPI-ESM-LR	MPI	component of MPI-OM	GR15	VP rheology, Semtner zero-layer, virtual ITD	3	3	Jungclaus et al. (2006)
MPI-ESM-MR	MPI	component of MPI-OM	GR15	VP rheology, Semtner zero-layer, virtual ITD	1	1	Jungclaus et al. (2006)
MRI-CGCM3	MRI	MRI.COM3			1	1	http://www.mri-jma.go.jp/Publish/Technical/DATA/VOL_64/tec_rep_mri_64.pdf
NorESM1-ME	NCC	CICE, v4		Energy-conserving thermo, ITD, EVP	1	1	Not available
NorESM1-ME	NCC	CICE, v4		Energy-conserving thermo, ITD, EVP	1	1	Not available

Note: this table has been filled with as much information as possible (July 2012).
A full documentation about the models is expected soon from the CMIP5 consortium.

Table 2. Inter-CMIP5 models correlations between five 1979–2010 Arctic sea ice predictors (I mean SSIE; II amplitude of the mean seasonal cycle of sea ice extent; III mean annual volume; IV mean sea ice extent of thin (0.01–0.5 m) ice in September; V linear trend in SSIE) and (LEFT) the 2030–2061 and 2069–2100 changes in SSIE with respect to 1979–2010 (RIGHT) the year at which SSIE drops below 1 and 4 million km^2 in September. Note that the number of models used for the calculation of correlations in the right part of the table can vary depending on the scenario and threshold (e.g. a limited number of models reach 1 million km^2 under RCP4.5 before 2100). The correlations are calculated using the mean of the members for multi-member models, and the single available member for the others.

	LEFT Predictand: SSIE anomalies at given time				RIGHT Predictand: year when SSIE drops below a threshold			
	RCP4.5		RCP8.5		RCP4.5		RCP8.5	
↓ Predictor ↓	2030–2061	2069–2100	2030–2061	2069–2100	1×10^6 km^2	4×10^6 km^2	1×10^6 km^2	4×10^6 km^2
(I) 1979–2010 mean SSIE	0.38[a]	0.20	0.38[a]	−0.62[c]	0.33[a]	0.89[c]	0.83[c]	0.96[c]
(II) 1979–2010 cycle ampl.	−0.06	0.05	−0.08	0.48[b]	−0.03	−0.41[a]	−0.41[a]	−0.58[c]
(III) 1979–2010 mean annual vol.	0.43[b]	0.15	0.39[a]	−0.52[b]	0.59[b]	0.72[c]	0.71[c]	0.76[c]
(IV) 1979–2010 mean thin ice ext.	−0.14	0.11	−0.10	0.40[a]	−0.40	−0.44[a]	−0.41[a]	−0.50[b]
(V) 1979–2010 trend SSIE	0.33[a]	0.29	0.46[b]	−0.35[a]	0.08	0.50[b]	0.65[c]	0.66[c]

Significant correlations at $p < 0.05$, $p < 0.01$ and $p < 0.001$ are marked with [a], [b] and [c], respectively.

TCD
6, 2931–2959, 2012

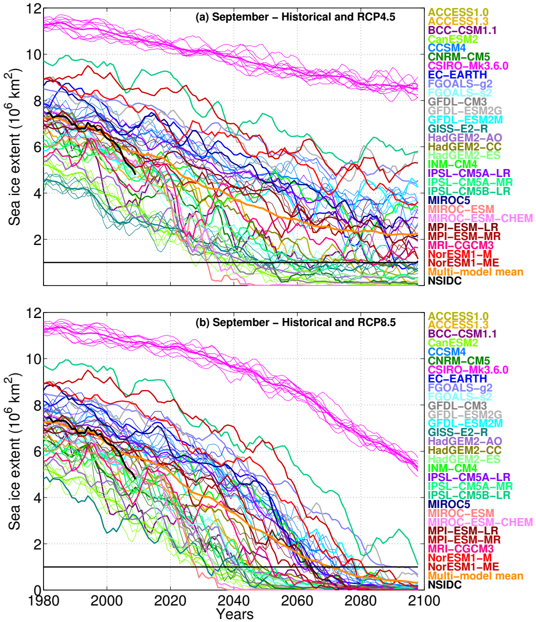

Fig. 1. September Arctic sea ice extent (5-yr running mean) as simulated by 29 CMIP5 models. The historical runs are merged with the RCPs (representative concentration pathways, Moss et al., 2010) 4.5 **(a)** and 8.5 **(b)** runs. Members of a same model, if any, are represented by thin lines. Individual models (or the mean of all their members, if any) are represented by thick lines. The multi-model mean (equal weight for each model) is depicted by the thick orange line. Observations (Fetterer et al., 2012) are shown as the thick black line. The horizontal black line marks the 1 million km^2 September sea ice extent threshold defining ice-free conditions in this paper.

TCD
6, 2931–2959, 2012

CMIP5 Arctic sea ice

F. Massonnet et al.

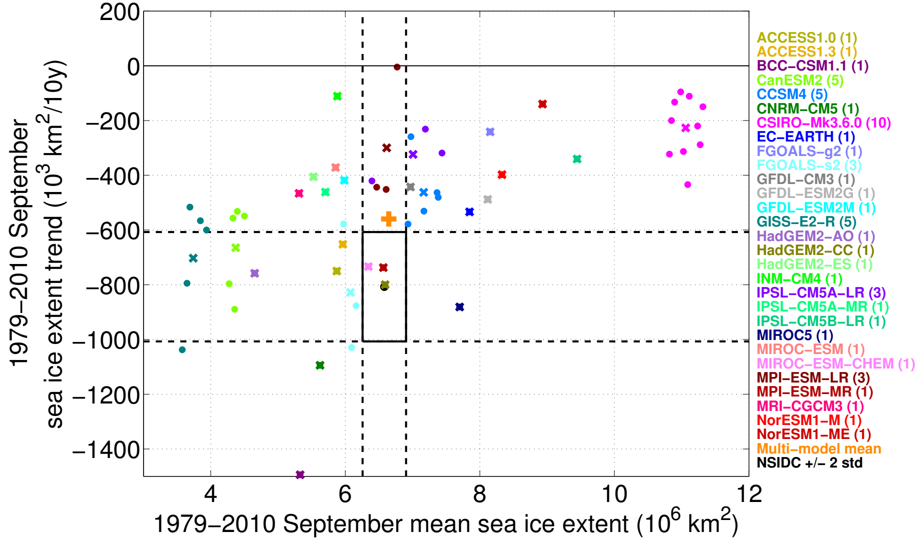

Fig. 2. 1979–2010 mean of (x-axis) and trend in (y-axis) September Arctic sea ice extent, as simulated by the CMIP5 models and their members. Members of a same model (if any) are represented by dots (•). Individual models (or the mean of all their members, if any) are represented by crosses (×). The number of members for each model is indicated in parentheses. The multi-model mean is depicted as the orange plus (+). Observations (Fetterer et al., 2012) are shown as the black dot, with $\pm 2\sigma$ windows for the mean and trend estimates (dashed lines). The values of σ are calculated as the standard deviation of the 1979–2010 SSIE time series divided by the square root of the number of observations (32) for the mean, and as the standard deviation estimate of the slope of the 1979–2010 SSIE linear fit.

TCD
6, 2931–2959, 2012

CMIP5 Arctic sea ice

F. Massonnet et al.

Title Page
Abstract | Introduction
Conclusions | References
Tables | Figures
◂◂ | ▸▸
◂ | ▸
Back | Close
Full Screen / Esc
Printer-friendly Version
Interactive Discussion

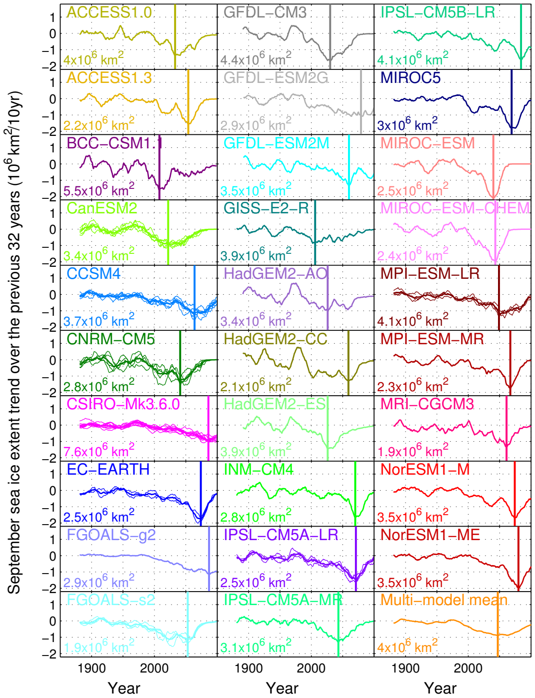

Fig. 3. Running trends (calculated on moving 32-yr windows) in SSIE under historical and RCP8.5 forcings. Members of a same model, if any, are represented by thin lines. Individual models (or the mean of all their members, if any) are represented by thick lines. The vertical line denotes the time at which the trend achieves its minimum, and the numbers at the lower-left of each panel is the mean SSIE at this time.

TCD
6, 2931–2959, 2012

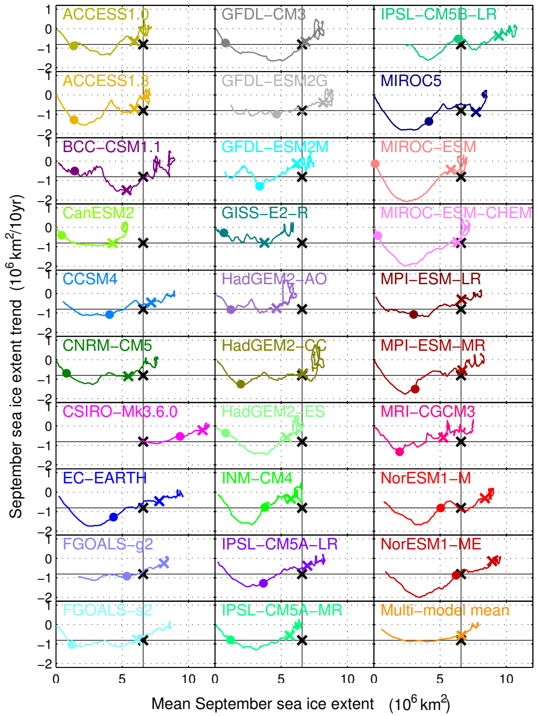

Fig. 4. Phase space of the SSIE as simulated by the CMIP5 models under RCP8.5: the mean SSIEs over consecutive 32-yr periods from 1850 to 2100 (x-axis) are plotted against the SSIE linear trends over the corresponding periods. The colored crosses indicate the current (1979–2010) position of the model on its trajectory. The colored dots are the model position over 2030–2061. The black cross is the current (1979–2010) state of the observed Arctic SSIE in this phase space. The reader can visualize a dynamic version of this figure at http://www.elic.ucl.ac.be/users/fmasson/CMIP5.gif (also available as Supplement).

TCD
6, 2931–2959, 2012

Title Page
Abstract
Introduction
Conclusions
References
Tables
Figures
◀
▶
Back
Close
Full Screen / Esc
Printer-friendly Version
Interactive Discussion

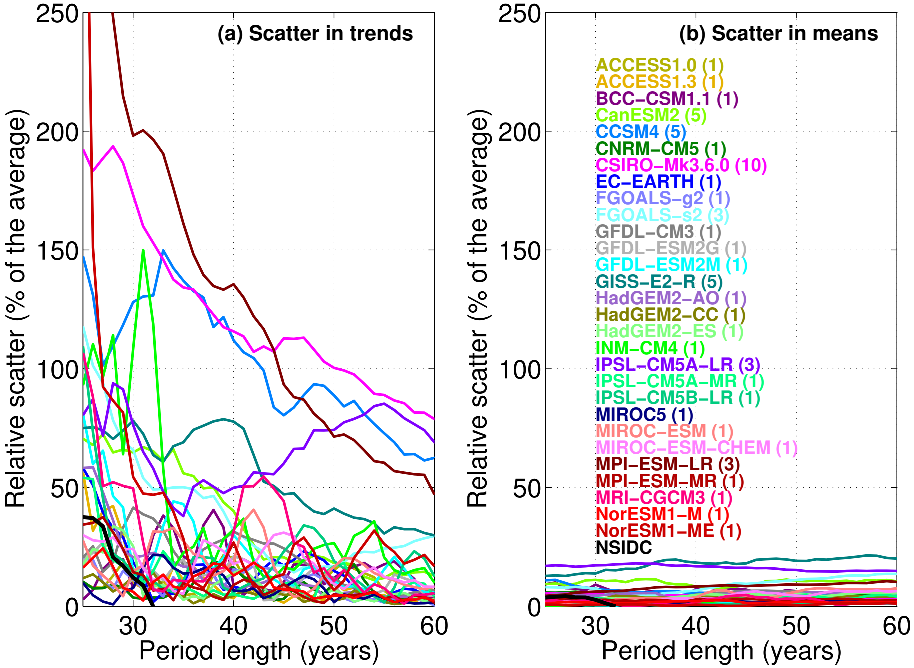

Fig. 5. Effects of internal variability on the trend in SSIE **(a)** and mean of SSIE **(b)** as a function of the length of the time series considered. For a given period length *x* (e.g. *x* = 30 yr), we construct 4 time intervals starting in 1979, 1980, 1981 and 1982 and ending *x* yr later (e.g. 1979–2009, 1980–2010, . . . , 1982–2012). The trends **(a)** and mean **(b)** SSIE are then calculated for all available members of the same model over these 4 time intervals. The relative spread in the sample (the range divided by the average) is displayed as the *y* coordinate. The observations (black) are treated like a model, but with one member (by definition), thus simply changing the end points.